

Phase Behavior of Polystyrene/Polybutadiene and Polystyrene/Hydrogenated Polybutadiene Mixtures: Effect of the Microstructure of Polybutadiene

Chang Dae Han* and Seung Bum Chun

Department of Polymer Engineering, The University of Akron, Akron, Ohio 44325

Stephen F. Hahn,*† Scott Q. Harper,†§ Philip J. Savickas,‡ and David M. Meunier‡

Central Research and Development and Analytical Sciences Laboratories, The Dow Chemical Company, Midland, Michigan 48674

Liang Li and Talat Yalcin

Department of Chemistry, University of Alberta, Edmonton, Alberta, Canada T6G 2G2

Received September 3, 1997; Revised Manuscript Received November 10, 1997

ABSTRACT: The effect of the microstructure on the phase behavior of mixtures of polybutadiene (PB) and poly(ethylene-*co*-1-butene) (PEB) with polystyrene (PS) has been investigated. A series of PBs with 1,2-addition content ranging from 7 to 93% were synthesized by anionic polymerization, and a portion of each was subsequently hydrogenated to yield PEB. Polymer pairs with blend compositions from 10 to 90 wt % were cast from toluene for each of the 16 PS/PB pairs and 7 PS/PEB pairs. Laser light scattering was used to obtain cloud point measurements, which were then used to construct phase diagrams. It was found that, for constituent components with equivalent degrees of polymerization, PS/PEB pairs give rise to higher upper critical solution temperatures than PS/PB pairs, indicating that PS/PEB pairs are less miscible than PS/PB pairs. Experimental phase diagrams were curve-fitted to theoretical phase diagrams predicted from the Flory–Huggins theory with the expression for the interaction parameter α : $\alpha = a + b/T + c\phi_{PS}/T$, where α is related to the Flory–Huggins interaction parameter χ by $\chi = \alpha V_r$, where V_r is the molar reference volume, T is the absolute temperature, and ϕ_{PS} is the volume fraction of PS in the mixture. α values for PS/PB mixtures increase with increasing 1,2-addition (miscibility decreases) while α values for PS/PEB mixtures decrease (miscibility increases) with increasing 1-butene content. Using these α values, the Helfand–Wasserman theory was applied to predict the order–disorder transition temperatures of PS-*block*-PB and PS-*block*-PEB copolymers with varying 1,2-addition and 1-butene content, respectively.

Introduction

In recent years, the tire industry has been successful in reducing the rolling resistance and increasing the traction of automobile tires by judiciously controlling the microstructures (1,2- and 1,4-addition) of polybutadiene (PB).¹ This can be easily understood from the point of view that PBs with different microstructure have vastly different glass transition temperatures (T_g s) and/or melting temperatures (T_m s), moduli, melt viscosities, and entanglement molecular weights.² For example, PB with 1,2-addition, having typically 25% crystallinity, has $T_g = -23$ °C and $T_m = \text{ca. } 90$ °C, whereas PB with 1,4-addition is an amorphous polymer with $T_g = -105$ °C. It is clear that different proportions of 1,2-addition versus 1,4-addition in a PB can give rise to vastly different physical and mechanical properties.² Another important use of PB is as a component in several of the most common multiphase polymer systems, including high-impact polystyrene (HIPS),³ poly(acrylonitrile-*stat*-butadiene-*stat*-styrene) (ABS polymer),⁴ and styrenic block copolymers.⁵ The function of

the compliant PB phase is influenced by the microstructure, which controls the modulus and glass transition behavior of that phase. In addition, the microstructure of the PB component has the potential to influence how phase separation occurs as these materials are prepared or the extent to which it exists in the final state. For this reason, microstructure and miscibility with common thermoplastic glassy phases represent an important design factor in these materials.

Although binary blends of PB and polystyrene (PS), owing to poor miscibility between the two, are not useful from a practical point of view, polystyrene-*block*-polybutadiene (SB diblock) and polystyrene-*block*-polybutadiene-*block*-polystyrene (SBS triblock) copolymers have long been used for polymer modification and other elastomer applications (e.g., shoe soles).⁵ Thus, in the past, the phase behavior of mixtures of PS and PB has been investigated extensively.^{6–9} To the best of our knowledge, however, little information is available in the literature as to how different microstructures of PB might affect its miscibility with PS. This represents an important variable in the design and synthesis of SB diblock and SBS triblock copolymers, because the microstructure of the PB block is expected to exert a great influence on the mechanical properties of these polymers.

PB is known to be thermally unstable, because cross-linking reactions can easily take place at an elevated

* To whom correspondence should be addressed.

† Central Research and Development, The Dow Chemical Company.

‡ Analytical Sciences Laboratories, The Dow Chemical Company.

§ Current address: Department of Human Genetics, University of Michigan, Ann Arbor, MI 48109-0618.

temperature. In order to improve thermal stability, PB may be hydrogenated, yielding poly(ethylene-*co*-1-butene) (PEB) from 1,2-addition and polyethylene from 1,4-addition. One successful commercial application of PEB can be found in the syntheses of PS-*block*-PEB (SEB diblock) and PS-*block*-PEB-*block*-PS (SEBS triblock) copolymers. To the best of our knowledge, there is little information available in the literature, which discusses the miscibility between PS and PEB with varying amounts of 1,2-addition in PB before being hydrogenated.

Very recently, we carried out an experimental investigation on the phase behavior of PS/PB and PS/PEB mixtures by synthesizing, via anionic polymerization, a series of PSs and PBs with varying amounts of 1,2-addition. Subsequently, a portion of each PB was hydrogenated to yield PEB. Upon preparation of PS/PB and PS/PEB mixtures with varying blend compositions, we conducted cloud point measurements, via laser light scattering, of the various mixtures to construct phase diagrams. We then determined, with the aid of the Flory-Huggins theory,^{10,11} the interaction parameter as a function of temperature and blend composition for PS/PB and PS/PEB pairs, respectively. We found that the interaction parameter depends greatly on the microstructure of PB in PS/PB or PS/PEB pairs. Using the interaction parameters thus determined, we predicted the order-disorder transition temperature (T_{ODT}) of SB or SEB block copolymers with varying 1,2-addition or 1-butene content. In this paper, we report the highlights of our findings.

Experimental Section

Materials and Sample Preparation. Two series of PB samples (molecular weights about 1000 and 3000, respectively) with varying amounts of 1,2-addition were synthesized by anionic polymerization.¹² Several PSs were also synthesized by anionic polymerization. Cyclohexane was purchased from Fisher Scientific and was passed over alumina prior to use. Tetrahydrofuran (THF) was purchased from Aldrich Chemical Company and was passed over activated alumina and Q5 catalyst beds prior to use. 1,3-Butadiene (CP grade) was purchased from Scott Specialty Gases and was passed over alumina, condensed into a transfer tube, and transferred to the reactor by nitrogen pressure. Tetramethylethylenediamine (TMEDA) was purchased from Aldrich Chemical Company and was distilled away from CaH_2 prior to use. Dipiperidinoethane (DIPIP) was prepared from piperidine and dibromoethane using the procedure of Miyahara et al.¹³ and was distilled under reduced pressure from CaH_2 prior to use. *sec*-Butyl lithium was obtained from the Lithium Corporation of America as a 12 wt % solution and was diluted with cyclohexane to 0.6 M prior to use. The concentration of active *sec*-butyl lithium was established using the Gilman double titration method.¹⁴

In a typical reaction, a 1500-mL glass tube reactor with screw-type agitator was cleaned and dried and then charged with 700 mL of dry cyclohexane. Dry THF was added by syringe as required. To this was added 46–49 g of 1,3-butadiene (passed over alumina) by transfer tube. The polymerization was initiated at 50 °C and was allowed to proceed at 55 °C. A polymerization exotherm of approximately 5 °C was typically observed. The polymerization was allowed to proceed for 60 min, after which termination was performed using 1 mL of degassed methanol. The polymer syrup was then drained from the reactor and was isolated by concentration on a rotary evaporator followed by precipitation of the polymer from methanol. 2,6-Di-*tert*-butyl-4-methylphenol (butylated hydroxytoluene, BHT) (0.5 g) was added to stabilize the polymer, which was then dried carefully in a vacuum oven at 50–60 °C. The microstructure was determined by ^1H

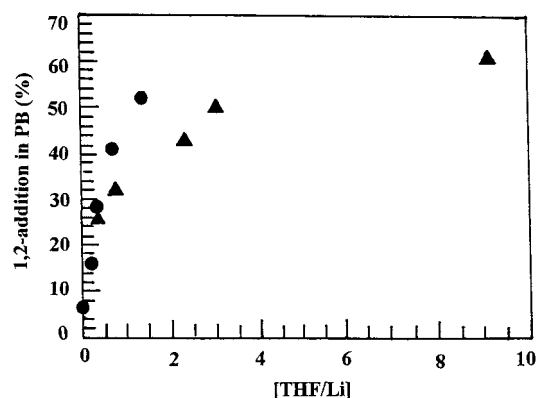


Figure 1. Variation of 1,2-addition with [THF]/[Li] ratio in polybutadiene synthesis in cyclohexane at ca. 0.02 M (▲) and ca. 0.045 M (●) Li concentration.

Table 1. Anionic Polymerization Conditions and Microstructure of Polybutadiene

sample code	[Li], g/mL	[base]/[Li]	base	1,2-addition, %	Mn, GPC
PB-93L	0.028	0.025	DIPIP	93	1100
PB-84L	0.042	neat THF	THF	84	1000
PB-75L	0.044	2.47	TMEDA	75	1000
PB-52L	0.052	1.53	THF	52	1200
PB-41L	0.047	0.86	THF	41	1150
PB-28L	0.044	0.42	THF	28	1200
PB-16L	0.043	0.27	THF	16	1350
PB-7L	0.030		none	7	1050
PB-84H	0.018	neat THF	TMEDA	84	2900
PB-78H	0.015	2.0	THF	78	3400
PB-61H	0.020	9.3	THF	61	3000
PB-50H	0.019	3.21	THF	50	3000
PB-43H	0.018	2.48	THF	43	3400
PB-32H	0.020	0.85	THF	32	3000
PB-26H	0.020	0.42	THF	26	3000
PB-7H	0.019		none	7	3400

nuclear magnetic resonance (NMR) spectroscopy in CDCl_3 ,¹⁵ and molecular weight was estimated with respect to PB standards by gel permeation chromatography (GPC) using THF as eluent and two Polymer Labs 5- μm mixed porosity columns with a differential refractometer detector.

The addition of Lewis bases such as ethers and amines to the anionic polymerization of butadiene with alkyl lithiums is known to increase the 1,2-addition in the resultant polymer.^{16,17} The Li concentration present in the polymerization, the nature of the Lewis base modifier, and the resultant 1,2-addition in the PBs prepared are summarized in Table 1. THF was used to prepare samples with 1,2-addition ranging from 7 to 84%. In the two series prepared here, the lower molecular weight PBs (having a higher Li concentration during polymerization) had a higher 1,2-addition for a [THF]/[Li] equivalent to that used to prepare the higher molecular weight PBs, as shown in Figure 1. Samples with high levels of 1,2-addition were prepared using TMEDA and DIPIP as the Lewis base. The relative amounts of *cis* and *trans* 1,4-additions were not determined. Table 2 gives a summary of the molecular weight data for PBs from GPC and mass spectral (MS) analysis, and Table 3 gives a summary of the molecular weight data for PSs from GPC.

The PB samples were saturated with hydrogen in a 1-L pressure reactor using a reduced Ni carboxylate catalyst.¹⁸ The hydrogenated polymer was characterized by ^1H NMR and GPC analysis. In all cases, no residual olefin was detected by NMR, and comparison of the GPC chromatogram before and after hydrogenation showed no change in polydispersity. Table 4 gives a summary of the molecular weight data for the PEBs samples used in this work; these values were determined on the basis of MS analysis of the parent PB samples. The hydrogenation of a 1,4-butadiene unit in PB provides a repeat unit which is equivalent to 2 mol of ethylene, while hydroge-

Table 2. Molecular Weight Data for Polybutadiene from GPC and Mass Spectral (MS) Analysis

sample code	M_w/M_n , GPC	M_n , MS	M_w , MS	M_w/M_n , MS
PB-93L	1.07	1408	1452	1.03
PB-84L	1.16	1465	1597	1.09
PB-75L	1.20	914	1080	1.18
PB-52L	1.07	1346	1404	1.04
PB-41L	1.08	1276	1338	1.05
PB-28L	1.07	1318	1379	1.05
PB-16L	1.07	1408	1468	1.04
PB-7L	1.07	1313	1372	1.05
PB-84H	1.06	3629	3738	1.03
PB-78H	1.04	4127	4191	1.02
PB-61H	1.07	3562	3684	1.04
PB-50H	1.07	3586	3674	1.02
PB-43H	1.05	3882	3963	1.02
PB-32H	1.06	3438	3514	1.02
PB-26H	1.06	3399	3481	1.02
PB-7H	1.05	3714	3793	1.02

Table 3. Molecular Weight Data for Anionic Polystyrene Samples

sample code	M_w , GPC	M_w/M_n , GPC
PS-3GY	2900	1.07
PS-4B	4300	1.05
PS-5J	5150	1.11
PS-6GY	6100	1.07
PS-1.5J	1500	1.11
PS-N1	1100	1.07

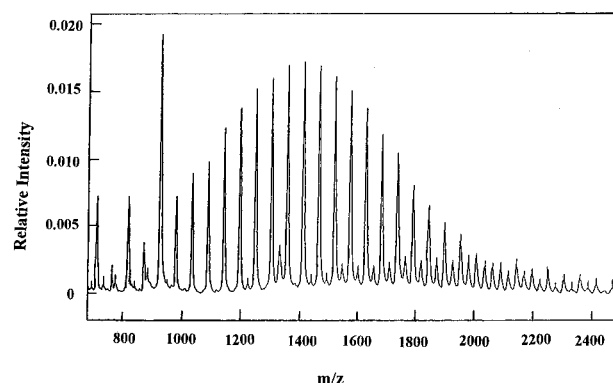
Table 4. Molecular Weight Data for Hydrogenated Polybutadienes

sample code	1-butene (wt %)	1-butene (mol %)	M_w , MS ^a
PEB-93L	93	87	1506
PEB-84L	84	72	1656
PEB-52L	52	35	1456
PEB-41L	41	26	1388
PEB-28L	28	16	1423
PEB-84H	84	72	3877
PEB-78H	78	64	4347

^a The values of molecular weight reported here are estimated from the molecular weight of PB determined from mass spectral analysis given in Table 2, based on complete hydrogenation of all double bonds in the PB.

nation of the 1,2-butadiene unit provides a repeat unit which is equivalent to 1 mol of 1-butene. For this reason, the molar ratio of 1,2- to 1,4-addition in PB will be different than the ethylene to 1-butene molar ratio in the PEB prepared from it. For simplicity the 1,2-addition content of the original polybutadiene sample is retained for the PEB sample code given in Table 4.

Due to the low molecular weight of the samples prepared here, and the difference between the microstructures of the samples made for this study and those used to calibrate the gel permeation chromatograph, molecular weights and molecular weight distributions obtained chromatographically were not thought to be sufficiently accurate. The PB samples were further characterized by matrix-assisted laser desorption/ionization mass spectrometry (MALDI-MS)^{19–21} to determine absolute molecular weight and molecular weight distribution. The polymer samples in the lower molecular weight series were analyzed on a home-built MALDI-MS linear time-of-flight instrument at the Dow Chemical Company using a GRAMS (Galactic) data system. The higher molecular weight PB samples were analyzed on a home-built time-lag focusing linear time-of-flight instrument at the University of Alberta. Mass spectra were collected using the Hewlett Packard MALDI software, and the data were further processed using the Igor Pro software Package (WaveMetrics). Both groups utilized a matrix consisting of *trans*-retinoic acid (TRA, Aldrich). The Dow group used silver acetylacetonate (Aldrich) as the cationizing agent, while the University of Alberta group used copper nitrate (J. T. Baker Chemical Co.). The target

**Figure 2.** MALDI-MS spectrum of PB-7L in the TRA/silver acetyl acetate matrix.

was then introduced into the mass spectrometer and desorbed with 337-nm laser pulses from a nitrogen laser. Approximately 400 pmol of polymer was applied to the target with the matrix in a molar ratio of about 200:1 matrix to analyte. About 10 nmol of cation was utilized. The mass scale was calibrated externally, the Dow group using Bovine Insulin (Sigma) and the Alberta group using monomethyl ether poly(ethylene glycol) 2000 (Sigma) as external standards.

Figure 2 shows the MALDI-MS spectrum of sample PB-7L in the TRA/silver acetylacetate matrix prepared by averaging 100 laser shots. The data were baseline-corrected using a linear two-point correction. Peaks at m/z 816 and 924 have direct mass interferences with the matrix; the intensities of the polymer ions for these peaks were estimated by linear interpolation of the peaks just preceding and just following these oligomers. About 30 oligomer peaks were included in each determination. A reproducibility study was performed on a sample of intermediate 1,2-addition (PB-52L) with four separate analyses. The analyses gave a molecular weight of 1383 Da, with a standard deviation of 18.5 Da (1.3% relative standard deviation). The polydispersities obtained for the PB samples using MALDI-MS are given in Table 2. In all cases the polydispersity measured by MALDI-MS is smaller than that determined by GPC analysis; this trend has been noted by other workers.²² Comparison of the two analytical techniques shows that GPC underestimates the molecular weight compared to MALDI-MS, and the difference is greater for samples with higher 1,2-addition.

Each of the PBs or PEBs synthesized was mixed with PS in toluene (ca. 10% solution), varying the weight fraction of PS from 0.1 to 0.9 in the binary mixture, and subsequently a few drops of the solution were placed on a glass slide for cloud point measurements. The solvent was evaporated very slowly first at room temperature in a fume hood and then in a vacuum oven at an elevated temperature. A summary of sample codes is given in Table 5 for the PS/PB pairs investigated and in Table 6 for the PS/PEB pairs investigated in this study.

Cloud Point Measurement. The cloud point of a specimen was determined using laser light scattering. Specifically, a glass slide containing a specimen was placed on the hot-stage of the sample holder attached with a programmable temperature controller. A low-power He–Ne laser (wavelength of 635 nm) was used as the light source, and a photodiode was used as the detector.

A specimen was first heated to a temperature slightly (ca. 20 °C) above the cloud point (i.e., in the isotropic region) followed by a slow cooling into the two-phase region where a change in light intensity was noticeable, and then the specimen was heated again at a preset rate (0.5–5 °C/min), during which information on both temperature and the intensity of scattered light was stored on a diskette. Figure 3 gives a typical result of such an experiment, namely, plots of temperature and the intensity of scattered light versus time during cooling and heating processes for a 50/50 PB-26H/PS-1.5J mixture. For each composition of a particular blend system, cloud point measurements were repeated three to five times

Table 5. Interaction Parameters Determined by Cloud Point Measurement for the PS/PB Pairs Investigated

sample code	1,2-addition in PB (%)	interaction parameter ^a	eq
PB-93L/PS-3GY	93	$\alpha = -0.1699 \times 10^{-2} + 1.0895/T + 0.0351\phi_{PS}/T$	6
PB-84L/PS-3GY	84	$\alpha = -0.1543 \times 10^{-2} + 0.9762/T + 0.0486\phi_{PS}/T$	7
PB-75L/PS-3GY	75	$\alpha = -0.2029 \times 10^{-2} + 1.2017/T + 0.1024\phi_{PS}/T$	8
PB-52L/PS-3GY	52	$\alpha = -0.2098 \times 10^{-2} + 1.1510/T + 0.0697\phi_{PS}/T$	9
PB-41L/PS-4B	41	$\alpha = -0.1814 \times 10^{-2} + 1.0480/T + 0.1138\phi_{PS}/T$	10
PB-28L/PS-4B	28	$\alpha = -0.1916 \times 10^{-2} + 1.0770/T + 0.0946\phi_{PS}/T$	11
PB-16L/PS-4B	16	$\alpha = -0.2038 \times 10^{-2} + 1.1020/T + 0.1266\phi_{PS}/T$	12
PB-7L/PS-4B	7	$\alpha = -0.1576 \times 10^{-2} + 0.9170/T + 0.0951\phi_{PS}/T$	13
PB-84H/PS-1.5J	84	$\alpha = -0.2388 \times 10^{-2} + 1.3550/T - 0.0186\phi_{PS}/T$	14
PB-78H/PS-1.5J	78	$\alpha = -0.1895 \times 10^{-2} + 1.1780/T - 0.0531\phi_{PS}/T$	15
PB-61H/PS-1.5J	61	$\alpha = -0.1790 \times 10^{-2} + 1.0830/T - 0.0332\phi_{PS}/T$	16
PB-50H/PS-1.5J	50	$\alpha = -0.1578 \times 10^{-2} + 1.0030/T - 0.0335\phi_{PS}/T$	17
PB-43H/PS-1.5J	43	$\alpha = -0.1436 \times 10^{-2} + 0.9401/T - 0.0329\phi_{PS}/T$	18
PB-32H/PS-1.5J	32	$\alpha = -0.1646 \times 10^{-2} + 0.9983/T - 0.0238\phi_{PS}/T$	19
PB-26H/PS-1.5J	26	$\alpha = -0.1847 \times 10^{-2} + 1.0560/T - 0.0091\phi_{PS}/T$	20
PB-7H/PS-1.5J	7	$\alpha = -0.1632 \times 10^{-2} + 0.9441/T + 0.0075\phi_{PS}/T$	21

^a The Flory–Huggins interaction parameter χ is related to α by $\chi = \alpha V_r$, where V_r is the molar volume of a reference component.

Table 6. Interaction Parameters Determined by Cloud Point Measurement for the PS/PEB Pairs Investigated

sample code	1-butene in PEB (wt %)	interaction parameter ^a	eq
PEB-93L/PS-N1	93	$\alpha = -0.6868 \times 10^{-2} + 3.3856/T + 0.0288\phi_{PS}/T$	22
PEB-84L/PS-N1	84	$\alpha = -0.7603 \times 10^{-2} + 3.6462/T + 0.0329\phi_{PS}/T$	23
PEB-52L/PS-N1	52	$\alpha = -0.5324 \times 10^{-2} + 2.7811/T + 0.0572\phi_{PS}/T$	24
PEB-41L/PS-N1	41	$\alpha = -0.5021 \times 10^{-2} + 2.6818/T + 0.0751\phi_{PS}/T$	25
PEB-28L/PS-N1	28	$\alpha = -0.4277 \times 10^{-2} + 2.3904/T + 0.0824\phi_{PS}/T$	26
PEB-84H/PS-N1	84	$\alpha = -0.1678 \times 10^{-2} + 1.2536/T - 0.0648\phi_{PS}/T$	27
PEB-78H/PS-N1	78	$\alpha = -0.2206 \times 10^{-2} + 1.6815/T - 0.2125\phi_{PS}/T$	28

^a The Flory–Huggins interaction parameter χ is related to α by $\chi = \alpha V_r$, where V_r is the molar volume of a reference component.

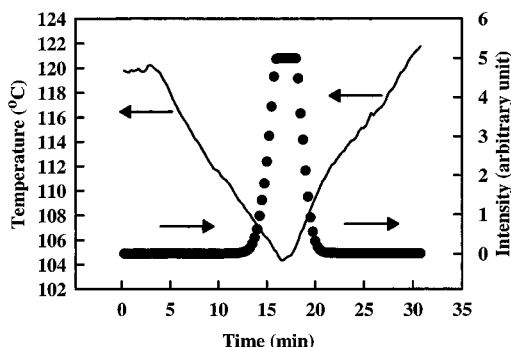


Figure 3. Temperature protocol employed and the corresponding intensity of scattered light during cooling and heating processes for cloud point measurement of the mixture consisting of 50 wt % PB-26H and 50 wt % PS-1.5J.

until data were reproducible, and a fresh specimen was used for each experimental run. For a given blend system, eight or nine compositions from 10/90 to 90/10 blend ratios were used to measure cloud point. Figure 4 gives a plot of the intensity of scattered light versus temperature during heating for a 50/50 PB-26H/PS-1.5J mixture. Similar plots were obtained for each of the eight or nine blend compositions, which then allowed us to construct a phase diagram, the results of which will be presented below.

We had to conduct a preliminary experiment for each PS/PB or PS/PEB pair, in order to determine an optimum range of the molecular weight of PS. We found that, for a given molecular weight of PB or PEB, PSs with molecular weights which were too low were not suitable for obtaining a reasonable phase diagram, while the upper critical solution temperature in PS/PEB mixtures exceeded the highest experimentally accessible temperature of 220 °C as the amount of 1-butene in PEB decreased. For this reason, we could not take cloud point measurements for PS/PEB pairs for PEB samples with low 1-butene content.

Results and Discussion

Phase Equilibria in PS/PB and PS/PEB Mixtures. Figure 5 gives phase diagrams for four PB/PS

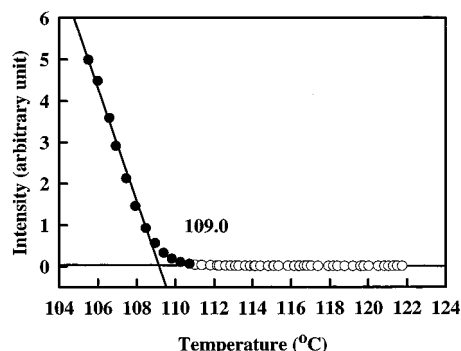


Figure 4. Plots of the intensity of scattered light versus temperature for the mixture consisting of 50 wt % PB-26H and 50 wt % PS-1.5J, which enabled us to determine the cloud point of 109 °C from the intersection of two straight lines.

pairs: (○) PB-7H/PS-1.5J mixtures; (Δ) PB-32H/PS-1.5J mixtures; (□) PB-50H/PS-1.5J mixtures; and (▽) PB-78H/PS-1.5J mixtures. Figure 6 gives phase diagrams for four other PB/PS pairs: (○) PB-26H/PS-1.5J mixtures; (Δ) PB-43H/PS-1.5J mixtures; (□) PB-61H/PS-1.5J mixtures; and (▽) PB-84H/PS-1.5J mixtures. The solid lines in Figures 5 and 6 describe phase diagrams predicted from the Flory–Huggins theory^{10–11} using the expressions for the interaction parameter α given in Table 5. Notice in Figures 5 and 6 that (i) all PB/PS pairs have about the same weight-average molecular weight (M_w) of PB ranging from 3500 to 4100 (hereafter will be referred to as high-molecular-weight PB) but different amounts of 1,2-addition in PB varying from 7 to 84% and that (ii) PS has the same molecular weight ($M_w = 1500$). It can be seen in Figures 5 and 6 that the phase diagram moves upward to a higher temperature as the amount of 1,2-addition in PB is increased. Thus we can conclude that miscibility between PS and PB decreases as the amount of 1,2-addition in PB increases. Below we will elaborate on the procedures employed to construct the predicted phase diagrams.

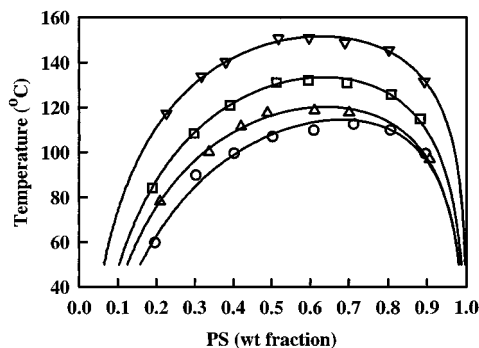


Figure 5. Phase diagrams for (○) PB-7H/PS-1.5J mixtures, (△) PB-32H/PS-1.5J mixtures, (□) PB-50H/PS-1.5J mixtures, and (▽) PB-78H/PS-1.5J mixtures. The solid lines represent theoretical predictions from a modified Flory–Huggins theory using the expression for the interaction parameter α given in Table 5.

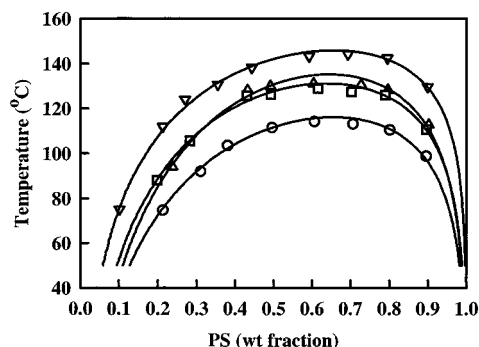


Figure 6. Phase diagrams for (○) PB-26H/PS-1.5J mixtures, (△) PB-43H/PS-1.5J mixtures, (□) PB-61H/PS-1.5J mixtures, and (▽) PB-84H/PS-1.5J mixtures. The solid lines represent theoretical predictions from a modified Flory–Huggins theory using the expression for the interaction parameter α given in Table 5.

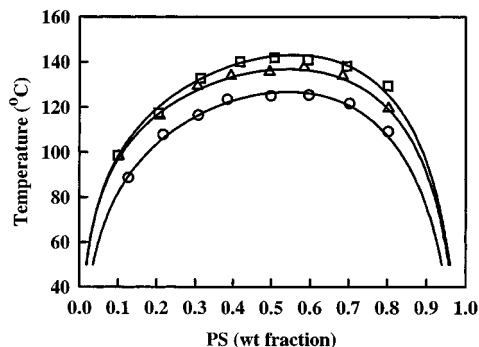


Figure 7. Phase diagrams for (○) PB-7L/PS-4B mixtures, (△) PB-28L/PS-4B mixtures, and (□) PB-41L/PS-4B mixtures. The solid lines represent theoretical predictions from a modified Flory–Huggins theory using the expression for the interaction parameter α given in Table 5.

Figure 7 gives phase diagrams for three PB/PS pairs: (○) PB-7L/PS-4B mixtures; (△) PB-28L/PS-4B mixtures; and (□) PB-41L/PS-4B mixtures. Figure 8 gives phase diagrams for four other PB/PS pairs: (○) PB-52L/PS-3GY mixtures; (△) PB-75L/PS-3GY mixtures; (□) PB-84L/PS-3GY mixtures; and (▽) PB-93L/PS-3GY mixtures. The solid lines in Figures 7 and 8 describe phase diagrams predicted from the Flory–Huggins theory using the expressions for the interaction parameter α given in Table 5. Notice in Figures 7 and 8 that (i) all PB/PS pairs have about the same values of M_w for PB ranging from 1300 to 1600 (hereafter will be referred to as low-molecular-weight PB) but different

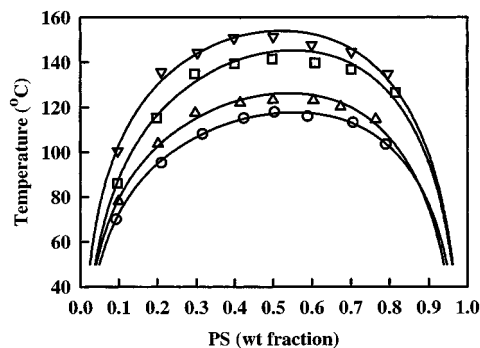


Figure 8. Phase diagrams for (○) PB-52L/PS-3GY mixtures, (△) PB-75L/PS-3GY mixtures, (□) PB-84L/PS-3G mixtures, and (▽) PB-93L/PS-3GY mixtures. The solid lines represent theoretical predictions from a modified Flory–Huggins theory using the expression for the interaction parameter α given in Table 5.

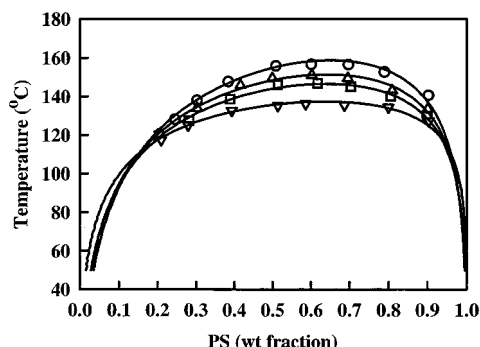


Figure 9. Phase diagrams for (○) PEB-28L/PS-N1 mixtures, (△) PEB-41L/PS-N1 mixtures, (□) PEB-52L/PS-N1 mixtures, and (▽) PEB-84L/PS-N1 mixtures. The solid lines represent theoretical predictions from a modified Flory–Huggins theory using the expression for the interaction parameter α given in Table 6.

amounts of 1,2-addition in PB varying from 7 to 93% and that (ii) PS has M_w varying from 2900 to 6100. It can be seen in Figures 7 and 8 that the phase diagram moves upward to a higher temperature as the amount of 1,2-addition in PB is increased, very similar to the case observed in Figures 5 and 6 for PS/PB mixtures having high-molecular-weight PBs.

Figure 9 gives phase diagrams for four PEB/PS pairs: (○) PEB-28L/PS-N1 mixtures; (△) PEB-41L/PS-N1 mixtures; (□) PEB-52L/PS-N1 mixtures; and (▽) PEB-84L/PS-N1 mixtures, in which the molecular weight of PEB ranges from 1400 to 1600 (hereafter will be referred to as low-molecular-weight PEB). Figure 10 gives phase diagrams for two other PEB/PS pairs: (○) PEB-78H/PS-N1 mixtures and (△) PEB-84H/PS-N1 mixtures, in which the molecular weight of PEB ranges from 3900 to 4300 (hereafter will be referred to as high-molecular-weight PEB). The solid lines in Figures 9 and 10 describe phase diagrams predicted from the Flory–Huggins theory^{10,11} using the expressions for the interaction parameter α given in Table 6. Notice in Figures 9 and 10 that (i) all PS/PEB mixtures had the same molecular weight (1100) of PS and that (ii) the critical temperature for PS/PEB pairs having high-molecular-weight PEB is much higher than that for PS/PEB pairs having low-molecular-weight PEB, suggesting that miscibility between PS and PEB decreases as the molecular weight of PEB increases.

What is of particular interest in Figures 9 and 10 is that the critical temperature decreases with increasing

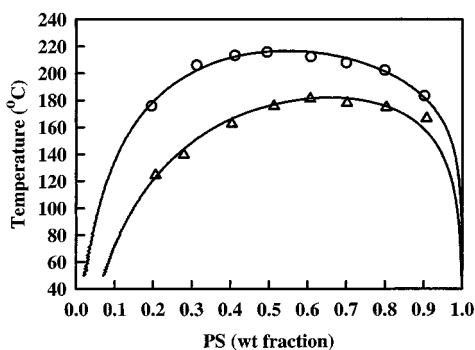


Figure 10. Phase diagrams for (○) PEB-78H/PS-N1 mixtures, and (△) PEB-84H/PS-N1 mixtures. The solid lines represent theoretical predictions from a modified Flory–Huggins theory using the expression for the interaction parameter α given in Table 6.

amounts of 1-butene in PEB, suggesting that the miscibility between PS and PEB increases with increasing amounts of 1-butene in PEB. This observation, which is opposite to that made above for PS/PB pairs, can be explained as follows. The hydrogenation of 1,2- and 1,4-addition in PB yields the equivalent of a random copolymer of 1-butene and ethylene. Since the miscibility between PS and poly(1-butene) (PB-1) is greater than that between PS and polyethylene (PE), the miscibility between PS and PEB will increase as the amount of 1,2-addition in PB increases, as this gives rise to a larger proportion of PB-1 than PE after hydrogenation.

Determination of the Interaction Parameter. The Gibbs free energy change during mixing of two liquids, ΔG_M , can be described by⁶

$$\Delta G_M = RT[(1/V_1)\phi_1 \ln \phi_1 + (1/V_2)\phi_2 \ln \phi_2] + \Lambda\phi_1\phi_2 \quad (1)$$

where ϕ_1 and ϕ_2 are the volume fractions of components 1 and 2, respectively, V_1 and V_2 are the molar volumes of components 1 and 2, respectively, R is the universal gas constant, T is the absolute temperature, and Λ denotes the interaction energy density, having the units of cal/cm³. For greater details of the theoretical background and physical description of eq 1, the readers are referred to a paper by Roe and Zin.⁶

It suffices to state that the quantity Λ in eq 1 depends, in general, on temperature, pressure, and composition of the mixture. According to Roe and Zin,⁶ Λ can be evaluated from eq 1 if the functional form of the dependence of Λ on temperature and composition is known. But there is no general rule about the dependence of Λ on temperature and composition. On the basis of experimental results, Roe and Zin⁶ used the following form:

$$\Lambda = \lambda_0 + \lambda_1\phi_1 + \lambda_T T \quad (2)$$

where λ_0 , λ_1 , and λ_T are constants that can be determined by the best fit to experimentally determined cloud points while solving eq 1 for a common tangent in the plot of ΔG_M versus ϕ_1 .

It is convenient to define the polymer–polymer interaction parameter α by $\alpha = \Lambda/RT$, which has the units of mol/cm³. Thus, eq 2 can be rewritten as

$$\alpha = A + B/T + C\phi_1/T \quad (3)$$

Often in the literature, the interaction parameter is also represented by the Flory–Huggins interaction param-

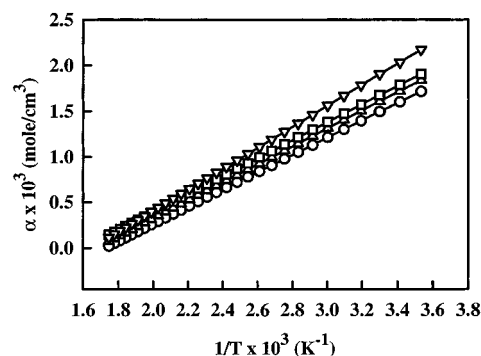


Figure 11. Plots of α versus $1/T$ for (○) a 50/50 PB-7H/PS-1.5J mixture (eq 21), (△) a 50/50 PB-32H/PS-1.5J mixture (eq 19), (□) a 50/50 PB-50H/PS-1.5J mixture (eq 17), and (▽) a 50/50 PB-78H/PS-1.5J mixture (eq 15).

eter χ , which is related to α by $\chi = \alpha V_r$, with V_r being the reference molar volume. It should be mentioned that there are different ways of defining V_r , for instance,

$$V_r = [M]_1 v_1 \quad (4)$$

or

$$V_r = [(M]_1 v_1)([M]_2 v_2)]^{1/2} \quad (5)$$

where $[M]_1$ and $[M]_2$ are the monomeric molecular weights of components 1 and 2, respectively, and v_1 and v_2 are the specific volumes of components 1 and 2, respectively. It is then clear that the numerical values of χ may vary with the definition of the reference volume chosen. It should be mentioned that the choice of the form given by eq 2 is rather arbitrary and, therefore, that other forms of the dependence of α (or χ) on temperature and composition have also been used.²³

In the present study, we used eq 3 to obtain expressions for α for PS/PB and PS/PEB mixtures, respectively, employed in our cloud point measurements. Table 5 gives a summary of the expressions of α for PS/PB mixtures, and Table 6 gives a summary of the expressions of α for PS/PEB mixtures.

In order to shed light on how differing amounts of 1,2-addition in PB might affect the temperature dependence of the interaction parameter α , Figure 11 gives plots of α versus the reciprocal temperature ($1/T$) for four PB/PS pairs at 50/50 blend composition: (○) 50/50 PB-7H/PS-1.5J mixture; (△) 50/50 PB-32H/PS-1.5J mixture; (□) 50/50 PB-50H/PS-1.5J mixture; and (▽) 50/50 PB-78H/PS-1.5J mixture. We observe from Figure 11 that the temperature dependence of α becomes stronger as the amount of 1,2-addition in PB increases. Figure 12 gives plots of α versus $1/T$ for three PS/PEB pairs at 50/50 blend composition: (○) 50/50 PEB-28L/PS-N1 mixture; (△) 50/50 PEB-52L/PS-N1 mixture; and (□) 50/50 PEB-84L/PS-N1 mixture. We observe from Figure 12 that the temperature dependence of α becomes stronger as the 1-butene content in PEB increases.

Prediction of the T_{ODTs} of SB and SEB Diblock Copolymers Using the Interaction Parameters Determined in This Study. As described in the Introduction, one of the motivations of the present study was to obtain information on the temperature dependence of the interaction parameters for PS/PB and PS/PEB pairs, respectively, which will then enable one to design, via the currently held theories, SB, SBS, SEB, or SEBS block copolymers with a target (or desired)

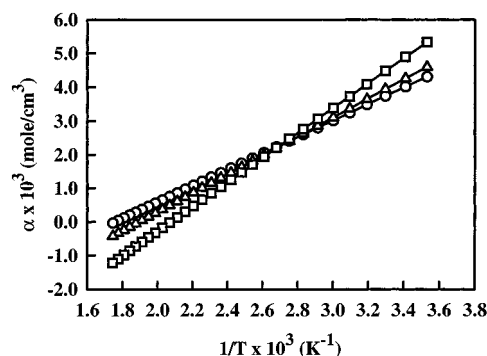


Figure 12. Plots of α versus $1/T$ for (O) a 50/50 PEB-28L/PS-N1 mixture (eq 26), (Δ) a 50/50 PEB-52L/PS-N1 mixture (eq 24), and (\square) a 50/50 PEB-84L/PS-N1 mixture (eq 23).

Table 7. Prediction of the T_{ODT} s of 8000PS-*block*-8000PB Copolymers Having Differing Amounts of 1,2-Addition in the PB Block

1,2-addition (%)	interaction parameter	T_{ODT} (°C)
93	eq 6	148
84	eq 7	129
75	eq 8	149
52	eq 9	116
41	eq 10	126
28	eq 11	119
16	eq 12	112
7	eq 13	107
84	eq 14	132
78	eq 15	135
61	eq 16	118
50	eq 17	119
43	eq 18	116
32	eq 19	107
26	eq 20	103
7	eq 21	93

Table 8. Prediction of the T_{ODT} s of 8000PS-*block*-8000PEB Copolymers Having Differing Amounts of 1-Butene in the PEB Block

1-butene (wt %)	interaction parameter	T_{ODT} (°C)
93	eq 22	164
84	eq 23	157
52	eq 24	178
41	eq 25	186
28	eq 26	193
84	eq 27	205
78	eq 28	244

T_{ODT} . Having determined the interaction parameters for PS/PB and PS/PEB pairs, we used the Helfand–Wasserman theory²⁴ to predict the T_{ODT} s of 8000PS-*block*-8000PB copolymers having varying amounts of 1,2-addition in the PB block and the T_{ODT} s of 8000PS-*block*-8000PEB copolymers having varying amounts of 1-butene in the PEB block. The results are summarized in Table 7 for 8000PS-*block*-8000PB copolymers and in Table 8 for 8000PS-*block*-8000PEB copolymers. In predicting the values of T_{ODT} given in Tables 7 and 8, we used the expressions for the temperature-dependent specific volume summarized in Table 9.

It is of interest to observe in Table 7 that the predicted T_{ODT} of the SB diblock copolymer increases with increasing amounts of 1,2-addition in the PB block, suggesting that the miscibility between PS and PB decreases with increasing amounts of 1,2-addition in the PB block. On the other hand, we observe in Table 8 that the predicted T_{ODT} of the SEB diblock copolymer decreases with increasing amounts of 1-butene in the PEB block, suggesting that the miscibility between PS

and PEB becomes greater with increasing amounts of 1-butene in the PEB block. The converse dependence between T_{ODT} and the amounts of 1,2-addition in the PB block or 1-butene content in the PEB block for SB and SEB diblock copolymers can be explained by the fact that the miscibility between PS and 1,2-PB is less than that between PS and 1,4-PB in the SB diblock copolymers, and the miscibility between PS and PE is less than that between PS and PB-1 in SEB diblock copolymers. This observation has significant influence on the strategy which might be taken in approaching the synthesis of SEB diblock or SEBS triblock copolymers.

Comparison of the Interaction Parameters Determined in This Study with the Literature. In order to compare the interaction parameters determined in this study (see Tables 5 and 6) with those in the literature, we decided to predict the T_{ODT} s of SB and SEB diblock copolymers. It turns out that there are only a few papers which reported on the experimental determination of the interaction parameters for PS/PB and PS/PEB pairs or the experimental determination of the T_{ODT} s of SB and SEB diblock copolymers.

Zin and Roe³¹ determined, via small-angle X-ray scattering (SAXS), the T_{ODT} of the 7000PS-*block*-21000PB copolymer, which had 30% 1,2-addition in the PB block, to be approximately 140 °C. As shown in Table 7 for SB diblock copolymers and in Table 8 for SEB block copolymers, the predicted T_{ODT} depends on the microstructure of the PB or PEB block. Since in the literature we could not find expressions of α for PS/PB pairs having 30% 1,2-addition in PB, we used the expressions for α , reported by Roe and Zin,⁶ for PS/PB pairs having 6% 1,2-addition in PB. This exercise was done to merely observe a trend. The expressions for α reported by Roe and Zin for PS/PB pairs having 6% 1,2-addition in PB and the predicted T_{ODT} , via the Helfand–Wasserman theory, of the 7000PS-*block*-21000PB copolymer are summarized in Table 10. Equations 35–38 in Table 10 were obtained³³ using $\alpha = \Lambda/RT$, since Roe and Zin⁶ reported the interaction energy density, Λ . Also given in Table 10, for comparison, is the predicted T_{ODT} , with the aid of eq 19 (for 32% 1,2-addition in PB) in Table 5, of the 7000PS-*block*-21000PB copolymer having 30% 1,2-addition in PB. Considering the experimental uncertainties associated with both the SAXS experiment and cloud point measurements and, also, the various assumptions made in the Helfand–Wasserman theory, we can conclude that agreement between prediction (124–149 °C) and experiment (140 °C) is very good.

There are only a few papers which reported on the experimental determination of the T_{ODT} of SEB diblock copolymers. Using SAXS, Owens et al.³⁴ determined the T_{ODT} to be 150 °C for an SEB diblock copolymer, which had $M_n = 19\,800$, $M_w/M_n = 1.08$, a 0.48 weight fraction of PS block, and a PEB block based on polybutadiene with 95% 1,2-addition. In the present study, for comparison, we calculated the T_{ODT} of this block copolymer to be 168 °C when using eq 23 and 176 °C when using eq 22. It is clear from these calculations that the predicted T_{ODT} depends on the microstructure and the molecular weight of PEB employed for obtaining α via cloud point measurements.

In 1971, using PS/PB mixtures having 20–25 wt % 1,2-addition in PB and PS/PI mixtures having 86–94 wt % 1,4-addition in PI, Rounds³⁵ obtained the following

Table 9. Expressions for Specific Volume Employed in This Study

material	specific volume (cm ³ /g)	eq	ref
PS	$v_{PS} = 0.9199 + 5.098 \times 10^{-4}(T - 273) + 2.354 \times 10^{-7}(T - 273)^2 + (32.46 + 0.1017(T - 273))/M_{w,PS}$	29	25
1,2-PB	$v_{12-PB} = 1.1072 + 8.19 \times 10^{-4}(T - 273)$	30	26, 27
1,4-PB	$v_{14-PB} = 1.1138 + 8.24 \times 10^{-4}(T - 273)$	31	28
PB-1	$v_{PB-1} = 1.134 + 7.003 \times 10^{-4}(T - 273)$	32	26, 27
PE	$v_{PE} = 1.2061 + 9.69 \times 10^{-4}(T - 406)$	33	29
PI	$v_{PI} = 1.0771 + 7.22 \times 10^{-4}(T - 273) + 2.46 \times 10^{-7}(T - 273)^2$	34	30

Table 10. Predicted T_{ODT} of the 7000PS-*block*-21000PB Copolymer Using the Interaction Parameters Obtained in This Study and by Roe et al.^{6,32}

expression for the interaction parameter	eq	ref	predicted T_{ODT} (°C)
$\alpha = -1.308 \times 10^{-3} + 0.8757/T - 0.0252\phi_{PS}/T$	35 ^a	6	124
$\alpha = -1.157 \times 10^{-3} + 0.8143/T + 0.0554\phi_{PS}/T$	36 ^b	6	137
$\alpha = -0.805 \times 10^{-3} + 0.6577/T + 0.1057\phi_{PS}/T$	37 ^c	6	131
$\alpha = -1.057 \times 10^{-3} + 0.7916/T + 0.0453\phi_{PS}/T$	38 ^d	32	142
$\alpha = -0.1646 \times 10^{-2} + 0.9983/T - 0.0238\phi_{PS}/T$	19 ^e	this study	148

^a For PS with $M_w = 2400$ and PB with $M_w = 2350$ and 6% 1,2-addition. ^b For PS with $M_w = 3500$ and PB with $M_w = 2350$ and 6% 1,2-addition. ^c For PS with $M_w = 5480$ and PB with $M_w = 2350$ and 6% 1,2-addition. ^d Later, Lin and Roe³² took an average of the three sets of cloud point measurements conducted previously by Roe and Zin.⁶ ^e For PS with $M_w = 1500$ and PB with $M_w = 3514$ and 32% 1,2-addition.

expression for α

$$\alpha = -0.0009 + 0.750/T \quad (39)$$

by averaging the cloud point measurements taken of the following polymer pairs: (i) PS/PI pair with $M_w = 2590$ for PS and $M_w = 4190$ for PI; (ii) PS/PI pair with $M_w = 4850$ for PS and $M_w = 1140$ for PI; (iii) PS/PB pair with $M_w = 4850$ for PS and $M_w = 1370$ for PB; and (iv) PS/PB pair with $M_w = 1720$ for PS and $M_w = 1370$ for PB. Rounds suggested that eq 39 be used to describe the miscibility of PS/PI or PS/PB pairs. Many investigators have subsequently made use of this suggestion. We have shown above that the interaction parameter α for PS/PB mixtures varies with the microstructure of PB, and therefore we are led to conclude that eq 39 cannot be regarded as being a general expression for all PS/PB pairs regardless of the microstructure of PB.

Concluding Remarks

In this study, using cloud point measurements we have obtained expressions for the interaction parameter for PS/PB and PS/PEB pairs, respectively, with varying microstructures of PB or PEB. To the best of our knowledge, at present such information (see Tables 5 and 6) is not available in the literature. For the study, a modified Flory–Huggins model was used to account for the concentration dependence of the interaction parameters.

To the best of our knowledge, there is little information available in the literature that discusses the miscibility between PS and PEB with varying amounts of 1,2-addition in PB before hydrogenation. That is, little information is available in the literature as to how different microstructures of PB might affect its miscibility with PS. This represents an important variable in the design and synthesis of SB diblock and SBS triblock copolymers, because the microstructure of the PB block is expected to exert a great influence on the mechanical properties of these polymers.

Most significantly, we have shown that the predicted T_{ODT} of the SB or SEB diblock copolymer depends on the microstructure of PB in the SB diblock copolymer or the microstructure of PEB in the SEB diblock copolymer. For example, in Table 7 we have shown that the T_{ODT} of 8000PS-*block*-8000PB copolymer is 107 °C when the PB block has 7% 1,2-addition and 148 °C when

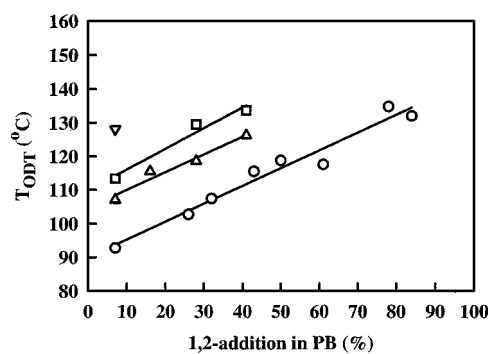


Figure 13. Effect of 1,2-addition in the PB block of the 8000PS-*block*-8000PB copolymer on T_{ODT} which was predicted from the Helfand–Wasserman theory, where solid lines are drawn through the predicted T_{ODT} s to guide the eye. Symbol \circ represents predicted T_{ODT} using the values of α for mixtures of high-molecular-weight PB (PB-7H through PB-84H) and PS-1.5J. Symbol Δ represents predicted T_{ODT} using the values of α for mixtures of low-molecular-weight PB (PB-7L, PB-16L, PB-28L, or PB-41L) and PS-4B. Symbol \square represents predicted T_{ODT} using the values of α for mixtures of low-molecular-weight PB (PB-7L, PB-28L, or PB-41L) and PS-5J. Symbol ∇ represents predicted T_{ODT} using the values of α for PB-7L/PS-6GY mixtures.

the PB block has 93% 1,2-addition. To elaborate on this further, we have prepared Figure 13, describing the effect of the amounts of 1,2-addition in the PB block on the predicted values of T_{ODT} for the 8000PS-*block*-8000PB copolymer. In reference to Figure 13, (i) the symbol \circ represents the predicted T_{ODT} of the 8000PS-*block*-8000PB copolymer having differing amounts of 1,2-addition in the PB block using the values of α determined from mixtures of high-molecular-weight PB (PB-7H through PB-84H) and PS-1.5J, (ii) the symbol Δ represents the predicted T_{ODT} of the 8000PS-*block*-8000PB copolymer having differing amounts of 1,2-addition in the PB block using the values of α determined from mixtures of low-molecular-weight PB (PB-7L, PB-16L, PB-28L, or PB-41L) and PS-4B, (iii) the symbol \square represents the predicted T_{ODT} of the 8000PS-*block*-8000PB copolymer having differing amounts of 1,2-addition in the PB block using the values of α determined from mixtures of low-molecular-weight PB (PB-7L, PB-28L, or PB-41L) and PS-5J, and (iv) the symbol ∇ represents the predicted T_{ODT} of the 8000PS-*block*-8000PB copolymer having 7% 1,2-addition in the

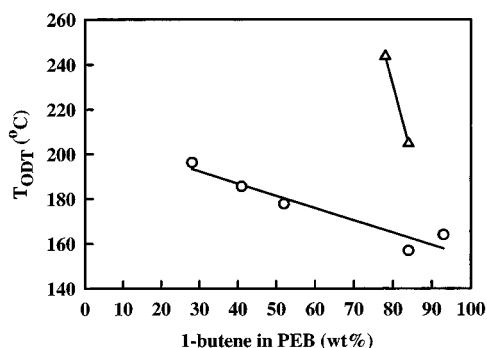


Figure 14. Effect of 1-butene in the PEB block of the 8000PS-*block*-8000PEB copolymer on T_{ODT} which was predicted from the Helfand–Wasserman theory, where solid lines are drawn through the predicted T_{ODT} s to guide the eye. Symbol \circ represents predicted T_{ODT} using the values of α for mixtures of low-molecular-weight PEB (PEB-28L, PEB-41L, PEB-52L, or PEB-84L) and PS-N1. Symbol Δ represents predicted T_{ODT} using the values of α for mixtures of high-molecular-weight PEB (PEB-78H or PEB-84H) and PS-N1.

PB block using the value of α determined from PB-7L/PS-6GY mixtures (see Table 5 for the expressions for α employed). It is clear from Figure 13 that the predicted T_{ODT} of the 8000PS-*block*-8000PB copolymer increases with increasing amounts of 1,2-addition in PB. The above observation reinforces our view that eq 39 cannot be regarded as being a general expression for all PS/PB mixtures or SB diblock copolymers regardless of the microdomain structure of PB.

On the other hand, in Figure 14 we observe that the predicted T_{ODT} of the 8000PS-*block*-8000PEB copolymer decreases with increasing amounts of 1-butene in the PEB block. In reference to Figure 14, the symbol \circ represents the predicted T_{ODT} of the 8000PS-*block*-8000PEB copolymer having differing amounts of 1-butene in PEB block using the values of α determined from mixtures of low-molecular-weight PEB (PEB-28L, PEB-41L, PEB-52L, or PEB-84L) and PS-N1, and the symbol Δ represents the predicted T_{ODT} of the 8000PS-*block*-8000PEB copolymer having differing amounts of 1-butene in the PEB block using the values of α determined from mixtures of high-molecular-weight PEB (PEB-78H or PEB-84H) and PS-N1 (see Table 6 for the expressions for α employed). The observed dependence of T_{ODT} on the amounts of 1-butene in PEB for the SEB diblock copolymer, shown in Figure 14, is of practical importance to the synthesis and design of SEB diblock copolymers for achieving a desired T_{ODT} . In view of the fact that values of α determined in this study for PS/PB and PS/PEB mixtures via cloud point measurement depend on the molecular weight of the constituent components, caution is necessary for predicting the miscibility of PS/PB or PS/PEB mixtures and the T_{ODT} s of SB or SEB diblock copolymers that have molecular weights higher than those employed in this study. Nevertheless, we sincerely hope that the expressions for the interaction parameter presented in Tables 5 and 6 will be useful to the synthesis and design of SB, SBS, SEB, or SEBS block copolymers with a desired T_{ODT} .

References and Notes

- (1) Halasa, A. F.; Massie, J. M. In *Kirk-Othmer Encyclopedia of Chemical Technology*, 4th ed.; Howe-Grant, M., Ed.; Wiley: New York, 1993; Vol. 8, p 1031 and references cited therein.
- (2) Carella, J. M.; Graessley, W. W.; Fetters, L. J. *Macromolecules* **1984**, *17*, 2775.
- (3) Echte, A. In *Rubber Toughened Plastics*; Riew, C. K., Ed.; Advances in Chemistry Series 222; American Chemical Society: Washington, DC, 1989.
- (4) Kulich, D. M.; Kelley, P. D.; Pace, J. E. In *Encyclopedia of Polymer Science and Engineering*, 2nd ed.; Mark, H. E., Bikales, N. M., Overberger, C. G., Menges, G., Kroschwitz, J. I., Eds.; Wiley: NY, 1989; Vol. 1, pp 388–426.
- (5) Holden, N. R.; Legge, N. R. In *Thermoplastic Elastomers*, 2nd ed.; Legge, N. R., Holden, G., Quirk, R. P., Schroeder, H. E., Eds.; Hanser: NY, 1996; Chapter 3.
- (6) Roe, R.-J.; Zin, W.-C. *Macromolecules* **1980**, *13*, 1221.
- (7) Lin, J. L.; Rigby, D.; Roe, R.-J. *Macromolecules* **1985**, *18*, 1609.
- (8) Hill, R. G.; Tomlins, P. E.; Higgins, J. S. *Polymer* **1985**, *26*, 1708.
- (9) Tasi, F.-J.; Torkelson, J. M. *Macromolecules* **1988**, *21*, 1026.
- (10) Flory, P. J. *J. Chem. Phys.* **1942**, *10*, 51.
- (11) Huggins, M. L. *J. Phys. Chem.* **1942**, *46*, 151; *Ann. N. Y. Acad. Soc.* **1942**, *41*, 1; *J. Am. Chem. Soc.* **1942**, *64*, 1712.
- (12) Halasa, A. F.; Lohr, D. F.; Hall, J. E. *J. Polym. Sci., Polym. Chem. Ed.* **1981**, *19*, 1357.
- (13) Miyahara, M.; Sueyoshi, S.; Kamiya, S. *Chem. Pharm. Bull.* **1985**, *33*, 5557.
- (14) Gilman, H.; Cartedge, F. K. *Organomet. Chem.* **1964**, *2*, 447.
- (15) Mochel, V. D. *Rubber Chem. Technol.* **1967**, *40*, 1200.
- (16) Hsieh, H. L.; Quirk, R. P. *Anionic Polymerization, Principles and Practical Applications*; Marcel Dekker: New York, 1996.
- (17) Morton, N.; Fetters, L. J. *Rubber Chem. Technol.* **1975**, *48*, 359.
- (18) Hahn, S. F. *J. Polym. Sci., Polym. Chem. Ed.* **1992**, *30*, 397.
- (19) Bahr, U.; Deppe, A.; Karas, M.; Hillenkamp, F. *Anal. Chem.* **1992**, *64*, 2866.
- (20) Whittall, R. M.; Li, L. *Anal. Chem.* **1995**, *67*, 1950.
- (21) Whittall, R. M.; Schriemer, D. C.; Li, L. *Anal. Chem.* **1997**, *69*, 2734.
- (22) Kassis, C. E.; DeSimone, J. M.; Linton, R. W.; Remsen, E. E.; Lange, G. W.; Friedman, R. M. *Rapid Commun. Mass Spectrosc.* **1997**, *11*, 1134.
- (23) Thudium, R. N.; Han, C. C. *Macromolecules* **1996**, *29*, 2143.
- (24) Helfand, E.; Wasserman, Z. R. In *Developments in Block Copolymers*; Goodman, I., Ed.; Applied Science: New York, 1982; Chapter 4.
- (25) Richardson, M. J.; Savill, N. G. *Polymer* **1977**, *18*, 3.
- (26) Bates, F. S.; Fetters, L. J.; Wignall, G. D. *Macromolecules* **1988**, *21*, 1086.
- (27) Gehlsen, M. D.; Bates, F. S. *Macromolecules* **1994**, *27*, 3611.
- (28) Rigby, D.; Roe, R.-J. *Macromolecules* **1986**, *19*, 721.
- (29) Zoller, P.; Walsh, D. J. In *Standard Pressure-Volume-Temperature Data for Polymers*; Technomic: Lancaster, PA, 1995; p 35. Regression analysis was taken of the data at temperatures above the melting point (406 K) at atmospheric pressure.
- (30) Han, C. D.; Kim, J.; Kim, J. K. *Macromolecules* **1989**, *22*, 383.
- (31) Zin, W.-C.; Roe, R.-J. *Macromolecules* **1984**, *17*, 183.
- (32) Lin, J.-L.; Roe, R.-J. *Macromolecules* **1987**, *20*, 2168.
- (33) The temperature T appearing in eq 2 of ref 6 has the units of Celsius. In order to maintain consistency with the interaction parameters summarized in Tables 5 and 6, T appearing in eqs 35–38 of Table 10 is expressed with the units of Kelvin.
- (34) Owens, J. N.; Gancarz, I. S.; Koberstein, J. T.; Russell, T. P. *Macromolecules* **1989**, *22*, 3380.
- (35) Rounds, N. A. *Thermodynamics and Phase Equilibria of Polystyrene-Polydiene Binary Mixtures*. Doctoral Dissertation, University of Akron, Akron, OH, 1971.

MA971309E